JACS
JOURNAL OF THE AMERICAN CHEMICAL SOCIETY

Communication

pubs.acs.org/JACS

Bifunctional Ag@Pd-Ag Nanocubes for Highly Sensitive Monitoring of Catalytic Reactions by Surface-Enhanced Raman Spectroscopy

Jumei Li,[†,‡] Jingyue Liu,[§] Yin Yang,[†] and Dong Qin*[,†]

[†]School of Materials Science and Engineering, Georgia Institute of Technology, Atlanta, Georgia 30332, United States
[‡]School of Materials Science and Engineering, Jingdezhen Ceramic Institute, Jingdezhen, Jiangxi 333403, PR China
[§]Department of Physics, Arizona State University, Tempe, Arizona 85287, United States

Supporting Information

ABSTRACT: We report a route to the facile synthesis of Ag@Pd-Ag nanocubes by cotitrating Na_2PdCl_4 and $AgNO_3$ into an aqueous suspension of Ag nanocubes at room temperature in the presence of ascorbic acid and poly(vinylpyrrolidone). With an increase in the total titration volume, we observed the codeposition of Pd and Ag atoms onto the edges, corners, and side faces of the Ag nanocubes in a site-by-site fashion. By maneuvering the Pd/Ag ratio, we could optimize the SERS and catalytic activities of the Ag@Pd-Ag nanocubes for in situ SERS monitoring of the Pd-catalyzed reduction of 4-nitrothiophenol by $NaBH_4$.

Noble-metal nanocrystals with well-defined shapes or facets have received significant attention as heterogeneous catalysts in recent years because of their remarkable activity and selectivity.[1] Most of these nanocrystals, however, cannot be combined with a spectroscopy method to measure the reaction kinetics and elucidate the mechanism by monitoring a catalytic reaction in situ.[2] Conceptually, surface-enhanced Raman spectroscopy (SERS) could serve as a powerful platform for the in situ monitoring of a catalytic reaction by developing bifunctional noble-metal nanocrystals with integration of SERS and catalytic activities. Among noble metals, it has been established that Ag and Au nanocrystals embrace strong localized surface plasmon resonance (LSPR) peaks in the visible region for SERS applications.[3] Many groups have demonstrated that Ag nanocubes with sharp corners and edges could enhance the Raman scattering cross section by 10^7−10^8-fold in terms of enhancement factor (EF).[4] Unfortunately, the reactions that could be catalyzed by Ag and Au nanocrystals are rather limited.[2b,5] In contrast, Pd and Pt nanocrystals are able to catalyze a larger number of chemical reactions,[6] but both Pd and Pt are extremely poor SERS substrates because of the very weak coupling between their free electrons and visible light.[7] The SERS EF of 40 nm Pd nanocubes is only 10^3−10^4, 10^4-fold weaker than that of similarly sized Ag nanocubes.[8] Taken together, it is extremely difficult to achieve the desired activities for both SERS and catalysis using monometallic Ag, Au, Pd, or Pt nanocrystals.

One approach to integrate SERS and catalytic properties on a single nanocrystal is to directly deposit Pd or Pt on surfaces of Au or Ag nanocrystals to form bimetallic nanocrystals with dual functionality. Many groups have made significant contributions to the fabrication of Au@Pd/Pt/Ag bifunctional nanocrystals by using Au as the core for SERS and a thin layer of Pd, Pt, or Ag as the shell for catalysis. Bifunctional nanocrystals were also demonstrated for in situ SERS monitoring of the reduction of 4-nitrothiophenol (4-NTP) to 4-aminothiophenol (4-ATP) by $NaBH_4$. Schlucker et al. reported the formation of Au@Pt/Au core/shell nanoscale raspberries by depositing Ag on Au nanoparticles, followed by galvanic replacement of Ag with a Pt or Au precursor.[2b] Han et al. demonstrated selective deposition of Au-Pd alloy at the ends of Au nanorods for generation of Au-Pd alloy horns.[9] Wang et al. created high-index facets of Ag on the surfaces of Au nanorods via selective deposition of Ag on the nanorods and selective chemical etching of Ag.[10] In contrast to their Au counterparts, the use of Ag nanocrystals has met limited success for the formation of Ag-Pd/Pt bifunctional nanocrystals because of galvanic replacement between elemental Ag and a Pd/Pt precursor.[11] Although the replacement reaction allows for the formation of Ag-Pd/Pt bimetallic hollow nanostructures with the catalytic properties associated with Pd/Pt atoms,[12] the significant loss of Ag content during galvanic replacement often leads to deterioration in SERS activity. Recently, we reported a strategy to complement galvanic replacement with coreduction by ascorbic acid (AA) for recovering galvanized Ag back to the surfaces of Ag nanocubes, ultimately obtaining Ag-Au hollow nanocubes with strong SERS activity.[13] Most recently, Wang et al. successfully demonstrated that a combination of galvanic replacement and coreduction by AA allowed for generation of Ag-Pd bimetallic hollow nanocubes with an edge length of 100 nm.[12b] They evaluated the catalytic activity of the Ag-Pd hollow nanostructures for the hydrogenation of *p*-nitrophenol by $NaBH_4$. Like others, they did not report the use of their Ag-Pd nanostructures for in situ SERS monitoring of a catalytic reaction, probably because of the lack of detection sensitivity.

Here we report the codeposition of Pd and Ag atoms onto the surfaces of Ag nanocubes for the generation of Ag@Pd-Ag nanocubes with integrated SERS and catalytic activities. Specifically, we cotitrated Na_2PdCl_4 and $AgNO_3$ into an aqueous suspension of Ag nanocubes in the presence of AA (reductant) and PVP (capping agent and colloidal stabilizer) at a slow injection rate at room temperature. We found that the galvanic reaction between Ag nanocubes and Na_2PdCl_4 was effectively suppressed because of the involvement of Ag^+ ions and AA,

Received: April 4, 2015
Published: May 21, 2015

DOI: 10.1021/jacs.5b03528
J. Am. Chem. Soc. 2015, 137, 7039−7042

leading to the codeposition of Pd and Ag atoms on the surfaces of Ag nanocubes in a site-by-site manner.[14] By increasing the total volume of precursor solutions added into the reaction system, we could control the growth pattern so that Pd and Ag atoms progressively deposited on the edges, corners, and then side faces of the Ag nanocubes. We confirmed that the catalytic activity of resultant Ag@Pd-Ag nanocubes could be manipulated by varying the amount of Pd deposited on the surfaces of nanocubes. Also, through inclusion of more Ag, we found that the Ag@Pd-Ag nanocubes embrace both LSPR and SERS properties similar to those of the original Ag cubes. By optimizing the ratio of Pd to Ag, we demonstrated the feasibility of using Ag@Pd-Ag nanocubes for in situ SERS monitoring of Pd-catalyzed reduction of 4-NTP by $NaBH_4$.

We first prepared Ag nanocubes with an edge length of 39.2 ± 1.6 nm, together with slight truncation at corners and edges (Figure S1). Next, we dispersed the Ag nanocubes in an aqueous solution containing AA and PVP, followed by cotitration of two precursor solutions, Na_2PdCl_4 and $AgNO_3$ (injection rate = 0.02 mL/min, under ambient conditions using a syringe pump). Figure 1A,C,E, shows TEM images of the products obtained after adding different volumes of the two precursor solutions. The corners and edges of the Ag nanocubes were sharpened, implying the preferential deposition of Pd and Ag atoms at these sites. With an increase in volume to 0.3 mL for each precursor solution, the edge length of the nanocubes increased to 41.5 ± 1.4 nm (Table S1). This suggests the formation of Ag@Pd-Ag nanocubes with shell thickness ≈ 1.1 nm. There was no void in each individual core/shell particle.

We also monitored the UV-vis spectra of the Ag nanocubes after reaction with different volumes of Na_2PdCl_4 and $AgNO_3$ (Figure S2A). During cotitration up to 0.3 mL for each precursor solution, the major LSPR peak of the nanocubes was only red-shifted from 436 to 445 nm, with slight broadening. This implies that the LSPR property of the original Ag nanocubes was well-preserved in the Ag@Pd-Ag nanocubes. To confirm deposition of Pd on Ag nanocubes, we used ICP-MS to measure Pd and Ag contents in the core/shell nanocubes. Pd content increased (2.2−7.3%) with the cotitration volume (0.1−0.5 mL, respectively; Table S2). We also used XPS to analyze the Pd deposited on the nanocubes (Figure S3). We found that the amount of Pd increased with the titration volume. Collectively, this suggests that we could control the amount of Pd deposited on the Ag nanocubes by varying the volume of Na_2PdCl_4 titrated into the reaction solution.

To resolve the distribution of Pd atoms on the surfaces of Ag nanocubes, we used 2.3% aqueous H_2O_2 to selectively remove the Ag component while leaving the Pd component intact. Figure 1B,D,F, shows TEM images of the resultant structures after selective etching of Ag templates with H_2O_2. At 0.1 mL, we observed formation of nanoframes with thin ridges and little coverage for the {111} facets at the corners (Figure 1B). As the volume increased to 0.2 and 0.3 mL, nanoframes with thicker ridges (Figure 1D) and nanocages (Figure 1F) were formed, respectively. We also collected aberration-corrected HAADF-STEM and EDS mapping images (Figure 1,G,H, respectively) from the nanocube to confirm that the Pd was mainly deposited on the edges and corners at a titration volume of 0.2 mL.

Figure 2 outlines the proposed pathways for deciphering the selective deposition of Pd and Ag atoms on a Ag nanocube.

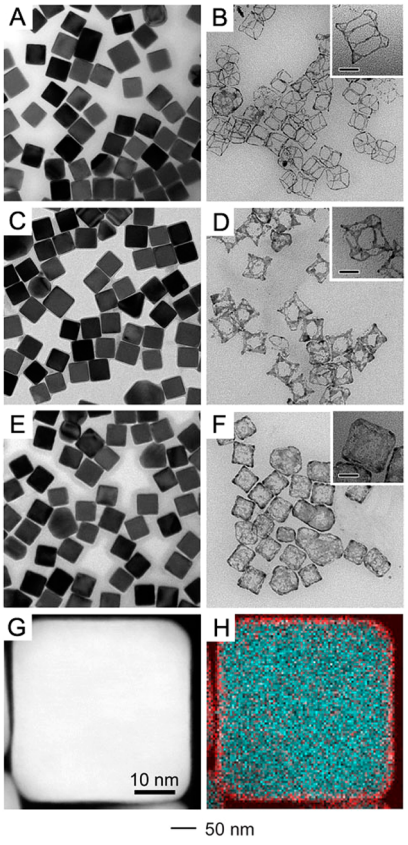

Figure 1. TEM images of Ag@Pd-Ag nanocubes (A, C, and E) before and (B, D, and F) after incubation with 2.3% H_2O_2. Samples were prepared by cotitrating different volumes of aqueous Na_2PdCl_4 and $AgNO_3$: (A and B) 0.1, (C and D) 0.2, and (E and F) 0.3 mL for each precursor. Scale bars in the insets are 20 nm. (G) HAADF-STEM and (H) EDS mapping images (red, Pd; blue, Ag) of a Ag@Pd-Ag nanocube shown in C.

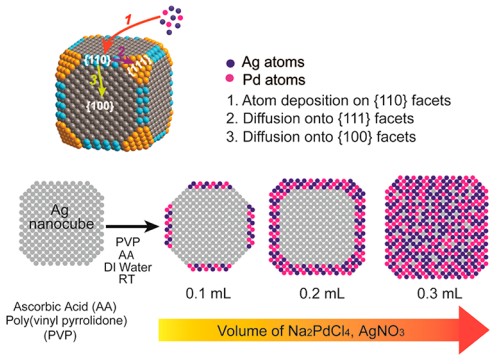

Figure 2. (top) Schematic illustration of proposed pathways for the selective deposition of Pd and Ag atoms onto different facets of a Ag nanocube whose {100} facets are capped by PVP. (bottom) Illustration (cross section along the front surface) of the transformation of a Ag nanocube into three types of Ag@Pd-Ag nanocubes when the volumes of the two precursors are increased.

Because it is difficult to resolve the deposition sites for the newly formed Ag atoms, we assumed that Pd and Ag atoms were deposited concomitantly. In principle, for metal nanocrystals with a face-centered cubic structure, the surface free energies of low-index facets increase on the order of $\gamma_{111} < \gamma_{100} < \gamma_{110}$. In our case, the selective passivation of {100} facets of Ag nanocubes by PVP would result in the reduction of γ_{100}, thus $\gamma_{100} < \gamma_{111} < \gamma_{110}$.

DOI: 10.1021/jacs.5b03528
J. Am. Chem. Soc. 2015, 137, 7039−7042

In the early stage of titration (e.g., 0.1 mL), the Pd and Ag atoms would preferentially nucleate on the high-energy {110} facets; these atoms would be largely confined to the edges of Ag nanocubes. This observation is consistent with previous findings in the synthesis of other bimetallic nanostructures.[15] As volumes of Pd and Ag precursors increased to 0.2 and 0.3 mL, respectively, more atoms were generated for their deposition onto the {110} facets, making the ridges thicker. Our data suggest that some atoms could sequentially migrate to the {111} facets (corners) and then {100} facets (side faces) of the Ag nanocubes by surface diffusion.[14,16]

We used 1,4-benzenedithiol (1,4-BDT) as a Raman probe to evaluate the SERS property of the Ag@Pd-Ag nanocubes. Figure 3A shows SERS spectra recorded from Ag nanocubes before and

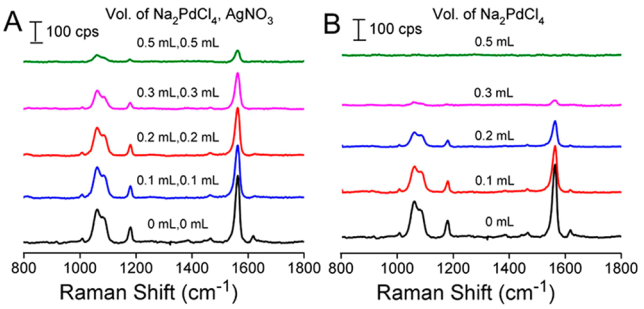

Figure 3. SERS spectra recorded from aqueous suspensions of nanocubes functionalized with 1,4-BDT molecules: (A) Ag@Pd-Ag nanocubes prepared with the cotitration of different volumes of Na_2PdCl_4 and $AgNO_3$, respectively, and (B) Ag@Pd nanocubes prepared by adding different volumes of Na_2PdCl_4 only.

after reaction with different volumes of Pd and Ag precursors. By monitoring the SERS peak at 1562 cm^{-1} (the benzene ring mode of 1,4-BDT), we found that its intensity dropped by 20, 30, 46, and 81% as the cotitration volume increased from 0.1 to 0.2, 0.3, and 0.5 mL, respectively. The data suggest that the deposition of Pd atoms on Ag nanocubes would deteriorate their SERS activity, consistent with previous findings.[8] Such a decrease might also arise from the less efficient adsorption of 1,4-BDT on Pd. We speculated that the Ag atoms deposited through the cotitration process could help to alleviate the damper effect of Pd on the LSPR and SERS properties of Ag nanocubes. To verify our hypothesis, we titrated Na_2PdCl_4 without the involvement of $AgNO_3$ while keeping all other experiential conditions unaltered. Figure S4A shows TEM image of the nanocubes after they had reacted with 0.2 mL of Na_2PdCl_4. Figure S4B indicates the formation of nanoframes upon etching with 2.3% H_2O_2, suggesting the selective deposition of Pd onto edges and corners of the Ag nanocubes. Figure S2B shows the UV-vis spectra of the Ag nanocubes before and after they had reacted with different volumes of $NaPdCl_4$. In this case, the LSPR of Ag nanocubes was slightly red-shifted from 436 to 439 and 443 nm at titration volumes of 0.1 and 0.2 mL, followed by a more significant redshift to 448 and 454 nm (together with great reduction in intensity) at titration volumes of 0.3 and 0.5 mL, respectively. We also collected SERS spectra from Ag@Pd nanocubes prepared by adding different volumes of $NaPdCl_4$. As shown in Figure 3B, the peak intensity at 1562 cm^{-1} was more drastically reduced by 39, 64, 93, and 100% as the titration volume increased from 0.1 to 0.2, 0.3, and 0.5 mL, respectively. On the basis of the band at 1562 cm^{-1}, we obtained SERS EFs of 2.2×10^5 and 1.1×10^5 for the Ag@Pd-Ag and Ag@Pd nanocubes that were prepared with a titration volume of 0.2 mL. (See the Supporting Information for details.) Collectively, our data suggest that it is essential to include Ag atoms during the deposition of Pd atoms to retain the SERS properties of the Ag nanocubes.

Next, we assessed the catalytic activity of the Ag@Pd-Ag nanocubes using the reduction of 4-nitrophenol (4-NP) to 4-aminophenol (4-AP) by $NaBH_4$.[12b,17] Specifically, we used UV-vis spectroscopy to monitor the decay of the absorption peak of 4-NP at 400 nm as reduction proceeded after adding a catalyst. Figure S5A shows the absorption spectra of 4-NP as a function of time when the reduction was catalyzed by Ag@Pd-Ag nanocubes prepared with a cotitration volume of 0.2 mL. We also benchmarked the performance of Ag@Pd-Ag nanocubes prepared with different cotitration volumes against the original Ag nanocubes at a fixed particle number of 1.5×10^{10}. Figure S5B shows the extinction (normalized to the initial value) at 400 nm as a function of time for the four catalysts: Ag nanocubes, Ag@Pd nanocubes prepared by adding 0.2 mL of Na_2PdCl_4, and Ag@Pd-Ag nanocubes obtained with cotitration volumes of 0.2 and 0.3 mL. The data confirmed that the Pd deposited on the Ag nanocubes could accelerate the reduction. The codeposition of Ag atoms during a cotitration process did not cause any significant change to the catalytic activity when comparing the two samples prepared using the same amount (e.g., 0.2 mL) of Na_2PdCl_4.

Finally, we leveraged the bifunctional property of the Ag@Pd-Ag nanocubes for in situ SERS monitoring of the Pd-catalyzed reduction of 4-NTP in a colloidal suspension. The nanocubes were prepared with a 0.2 mL cotitration volume, then incubated with a 4-NTP solution. After surface functionalization, we recorded a UV-vis spectrum for the functionalized nanocubes (Figure S6); it was essentially identical to that of the as-prepared nanocubes. This confirms the preservation of sharpness for the corners and edges during surface functionalization. We then added $NaBH_4$ into the colloidal suspension to initiate the catalytic reaction, followed by the collection of SERS spectra at different reaction times. At t = 0, Figure 4A shows the SERS

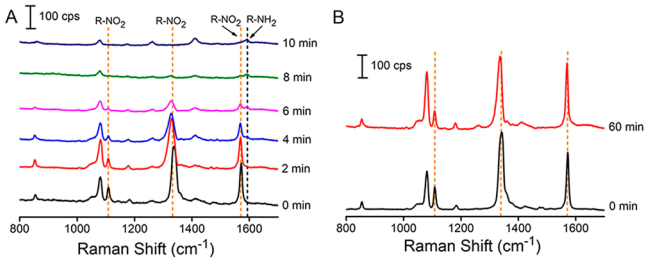

Figure 4. SERS spectra recorded during the reduction of 4-NTP to 4-ATP catalyzed by the (A) Ag@Pd-Ag nanocubes and (B) Ag nanocubes in the presence of $NaBH_4$. The R-NO_2 and R-NH_2 represent the 4-NTP and 4-ATP, respectively.

spectrum of 4-NTP with three characteristic vibrational bands (dashed orange lines) at 1108 cm^{-1} (O−N−O stretching), 1336 cm^{-1} (O−N−O stretching), and 1572 cm^{-1} (phenol-ring mode).[9] As the reaction progressed, the intensities of these bands decreased progressively in 10 min with the concomitant emergence of a new band corresponding to the phenol-ring mode of 4-ATP at 1591 cm^{-1} (dashed black line). It is worth noting that the other vibrational modes shown in the SERS spectra can also be assigned to those shown in the Raman spectra of 4-NTP and 4-ATP (Figure S7 and Table S3). To rule out the photoinduced reduction of 4-NTP to 4-ATP, we recorded the

DOI: 10.1021/jacs.5b03528
J. Am. Chem. Soc. 2015, 137, 7039−7042

time-dependent SERS spectra of the 4-NTP-functionalized cubes in the absence of $NaBH_4$ upon continuous laser irradiation. As shown in Figure S8, the SERS spectra remained the same after the illumination with 532 nm laser for 30 min. We also used in situ SERS to monitor the reduction of 4-NTP in the presence of Ag nanocubes as a catalyst (Figure 4B). After 60 min, the SERS spectra remained essentially the same, indicating that the Ag nanocubes were unable to catalyze this reaction. We also used the Ag@Pd nanocubes for in situ SERS. We found that only the cubes with Pd deposited on the surfaces could also accelerate the reaction rate (Figure S9). However, the SERS peak intensities were weaker compared to those of the Ag@Pd-Ag nanocubes, which is consistent with Figure 3B.

In principle, SERS could be used to identify the species that bind to the surface of the cubes during the reduction of 4-NTP by $NaBH_4$. As shown in Figure 4A, the reduction occurred too quickly to give the signatures of 4,4′-dimercaptoazobenzene (DMAB), an intermediate. By reducing the amount of $NaBH_4$ involved in the reaction, however, we observed the formation of DMAB (Figure S10), suggesting that the Pd-catalyzed reduction proceeded by a two-step mechanism.[2b,10] Additionally, we noticed that the intensity of band at 1589 cm^{-1} for 4-ATP was ~7.2 times weaker than the band at 1572 cm^{-1} for 4-NTP. On the basis of the SERS of 4-NTP and 4-ATP adsorbed on the Ag@Pd-Ag nanocubes, the difference should only be 2.6 times (Figure S11), indicating possible desorption of ATP from the surface. Although we did not obtain Raman signals of 4-ATP from the reaction solution after removing nanocubes (Figure S12), we studied the desorption issue by monitoring the SERS of 4-ATP on the Ag@Pd-Ag nanocubes upon adding $NaBH_4$ (Figure S13). The SERS intensity dropped by 80%, followed by no change for 30 min. The data suggest the desorption of ATP from the surface of nanocubes as a result of a stronger binding of BH_4^- to the surface of the nanocubes.[18]

We have demonstrated a facile synthesis of Ag@Pd-Ag nanocubes through the cotitration of Na_2PdCl_4 and $AgNO_3$ into an aqueous suspension of Ag nanocubes in the presence of AA and PVP. We discovered that the Pd and Ag atoms were initially deposited on the edges, followed by surface diffusion to the corners and side faces of nanocubes. By simply controlling the titrated volumes of Pd and Ag precursors, we could control the ratio of Pd to Ag, and ultimately, integrate the optimal SERS and catalytic properties into a single nanocube for highly sensitive monitoring of Pd-catalytic reactions by SERS.

■ ASSOCIATED CONTENT

Supporting Information

Experimental details and data. The Supporting Information is available free of charge on the ACS Publications website at DOI: 10.1021/jacs.5b03528.

■ AUTHOR INFORMATION

Corresponding Author

*dong.qin@mse.gatech.edu

Notes

The authors declare no competing financial interest.

■ ACKNOWLEDGMENTS

We thank Georgia Tech for start-up funds. We thank Ming Luo and Hsin-Chieh Peng for performing the ICP-MS and XPS analyses. J. L. was supported by the start-up fund from Arizona State University (ASU). We acknowledge the use of facilities in the John M. Cowley Center for High Resolution Electron Microscopy at ASU.

■ REFERENCES

(1) (a) Habas, S. E.; Lee, H.; Radmilovic, V.; Somorjai, G. A.; Yang, P. *Nat. Mater.* **2007**, *6*, 692. (b) Ruditskiy, A.; Choi, S.; Peng, H.-C.; Xia, Y. *MRS Bull.* **2014**, *39*, 727. (c) Burda, C.; Chen, X.; Narayanan, R.; El-Sayed, M. A. *Chem. Rev.* **2005**, *105*, 1025. (d) Hu, Y.; Liu, Y.; Sun, Y. *Adv. Funct. Mater.* **2015**, *25*, 1638.

(2) (a) Heck, K. N.; Janesko, B. G.; Scuseria, G. E.; Halas, N. J.; Wong, M. S. *J. Am. Chem. Soc.* **2008**, *130*, 16592. (b) Xie, W.; Herrmann, C.; Kompe, K.; Haase, M.; Schlucker, S. *J. Am. Chem. Soc.* **2011**, *133*, 19302. (c) Joseph, V.; Engelbrekt, C.; Zhang, J.; Gernert, U.; Ulstrup, J.; Kneipp, J. *Angew. Chem., Int. Ed.* **2012**, *51*, 7592.

(3) (a) Kneipp, K.; Kneipp, H.; Itzkan, I.; Dasari, R. R.; Feld, M. S. *Chem. Rev.* **1999**, *99*, 2957. (b) Rycenga, M.; Cobley, C. M.; Zeng, J.; Li, W.; Moran, C. H.; Zhang, Q.; Qin, D.; Xia, Y. *Chem. Rev.* **2011**, *111*, 3669. (c) Zhang, Q.; Li, W.; Moran, C.; Zeng, J.; Chen, J.; Wen, L.-P.; Xia, Y. *J. Am. Chem. Soc.* **2010**, *132*, 11372. (d) Jones, M. R.; Osberg, K. D.; Macfarlane, R. J.; Langille, M. R.; Mirkin, C. A. *Chem. Rev.* **2011**, *111*, 3736. (e) Xia, Y.; Xiong, Y.; Lim, B.; Skrabalak, S. E. *Angew. Chem., Int. Ed.* **2009**, *48*, 60. (f) Yang, Y.; Liu, J.; Fu, Z.; Qin, D. *J. Am. Chem. Soc.* **2014**, *136*, 8153. (g) Samal, A. K.; Polavarapu, L.; Rodal-Cedeira, S.; Liz-Marzán, L. M.; Pérez-Juste, J.; Pastoriza-Santos, I. *Langmuir* **2013**, *29*, 15076.

(4) (a) McLellan, J. M.; Li, Z.-Y.; Siekkinen, A. R.; Xia, Y. *Nano Lett.* **2007**, *7*, 1013. (b) Rycenga, M.; Xia, X.; Moran, C. H.; Zhou, F.; Qin, D.; Li, Z.-Y.; Xia, Y. *Angew. Chem., Int. Ed.* **2011**, *50*, 5473.

(5) Cai, W.; Tang, X.; Sun, B.; Yang, L. *Nanoscale* **2014**, *6*, 7954.

(6) (a) Wu, J. B.; Yang, H. *Acc. Chem. Res.* **2013**, *46*, 1848. (b) Zhang, H.; Jin, M.; Xia, Y. *Chem. Soc. Rev.* **2012**, *41*, 8035. (c) Guo, S.; Zhang, X.; Zhu, W.; He, K.; Su, D.; Mendoza-Garcia, A.; Ho, S. F.; Lu, G.; Sun, S. *J. Am. Chem. Soc.* **2014**, *136*, 15026.

(7) (a) Zhang, Y.; Gao, X.; Weaver, M. J. *J. Phys. Chem.* **1993**, *97*, 8656. (b) Tian, Z.-Q.; Ren, B.; Li, J.-F.; Yang, Z.-L. *Chem. Commun.* **2007**, *34*, 3514.

(8) McLellan, J. M.; Xiong, Y.; Hu, M.; Xia, Y. *Chem. Phys. Lett.* **2006**, *417*, 230.

(9) Huang, J.; Zhu, Y.; Lin, M.; Wang, Q.; Zhao, L.; Yang, Y.; Yao, K. X.; Han, Y. *J. Am. Chem. Soc.* **2013**, *135*, 8552.

(10) Jing, H.; Zhang, Q.; Large, N.; Yu, C.; Blom, D. A.; Nordlander, P.; Wang, H. *Nano Lett.* **2014**, *14*, 3674.

(11) Xia, X.; Wang, Y.; Ruditskiy, A.; Xia, Y. *Adv. Mater.* **2013**, *25*, 6313.

(12) (a) Zhang, H.; Jin, M.; Liu, H.; Wang, J.; Kim, M. J.; Yang, D.; Xie, Z.; Liu, J.; Xia, Y. *ACS Nano* **2011**, *5*, 8212. (b) Jing, H.; Wang, H. *Chem. Mater.* **2015**, *27*, 2172. (c) Mahmoud, M. A.; El-Sayed, M. A. *Langmuir* **2012**, *28*, 4051. (d) Zhang, W.; Yang, J.; Lu, X. *ACS Nano* **2012**, *6*, 7397.

(13) Yang, Y.; Zhang, Q.; Fu, Z.-W.; Qin, D. *ACS Appl. Mater. Interfaces* **2014**, *6*, 3750.

(14) (a) Xia, X.; Xie, S.; Liu, M.; Peng, H.-C.; Lu, N.; Wang, J.; Kim, M. J.; Xia, Y. *Proc. Natl. Acad. Sci. U.S.A.* **2013**, *110*, 6669. (b) DeSantis, C. J.; Peverly, A. A.; Peters, D. G.; Skrabalak, S. E. *Nano Lett.* **2011**, *11*, 2164.

(15) (a) Xia, X.; Zeng, J.; Oetjen, L. K.; Li, Q.; Xia, Y. *J. Am. Chem. Soc.* **2012**, *134*, 1793. (b) Zhang, L.; Niu, W.; Gao, W.; Qi, L.; Lai, J.; Zhao, J.; Xu, G. *ACS Nano* **2014**, *8*, 5953. (c) Wu, Y.; Wang, D.; Zhou, G.; Yu, R.; Chen, C.; Li, Y. *J. Am. Chem. Soc.* **2014**, *136*, 11594.

(16) (a) Rigby, S. P. *Langmuir* **2003**, *19*, 364. (b) Weber, D.; Sederman, A. J.; Mantle, M. D.; Gladden, L. F. *Phys. Chem. Chem. Phys.* **2010**, *12*, 2619. (c) Zhan, D.; Velmurugan, J.; Mirkin, M. V. *J. Am. Chem. Soc.* **2009**, *131*, 14756.

(17) (a) Halder, K. K.; Kundu, S.; Patra, A. *ACS Appl. Mater. Interfaces* **2014**, *6*, 21946. (b) Hervés, P.; Pérez-Lorenzo, M.; Liz-Marzán, L. M.; Dzubiella, J.; Lu, Y.; Ballauff, M. *Chem. Soc. Rev.* **2012**, *41*, 5577. (c) Aditya, T.; Pal, A.; Pal, T. *Chem. Commun.* **2015**, *51*, 9410.

(18) Ansar, S. M.; Ameer, F. S.; Hu, W.; Zou, S.; Pittman, C. U.; Zhang, D. *Nano Lett.* **2013**, *13*, 1226.

DOI: 10.1021/jacs.5b03528
J. Am. Chem. Soc. 2015, 137, 7039−7042